ACS Infectious Diseases

pubs.acs.org/journal/aidcbc

Letter

The Structure-Based Design of SARS-CoV-2 nsp14 Methyltransferase Ligands Yields Nanomolar Inhibitors

Tomáš Otava, Michal Šála, Fengling Li, Jindřich Fanfrlík, Kanchan Devkota, Sumera Perveen, Irene Chau, Paknoosh Pakarian, Pavel Hobza, Masoud Vedadi,* Evzen Boura,* and Radim Nencka*

Cite This: https://doi.org/10.1021/acsinfecdis.1c00131

Read Online

ACCESS | Metrics & More | Article Recommendations | Supporting Information

ABSTRACT: In this study, we have focused on the structure-based design of the inhibitors of one of the two SARS-CoV-2 methyltransferases (MTases), nsp14. This MTase catalyzes the transfer of the methyl group from *S*-adenosyl-L-methionine (SAM) to cap the guanosine triphosphate moiety of the newly synthesized viral RNA, yielding the methylated capped RNA and *S*-adenosyl-L-homocysteine (SAH). As the crystal structure of SARS-CoV-2 nsp14 is unknown, we have taken advantage of its high homology to SARS-CoV nsp14 and prepared its homology model, which has allowed us to identify novel SAH derivatives modified at the adenine nucleobase as inhibitors of this important viral target. We have synthesized and tested the designed compounds in vitro and shown that these derivatives exert unprecedented inhibitory activity against this crucial enzyme. The docking studies nicely explain the contribution of an aromatic part attached by a linker to the position 7 of the 7-deaza analogues of SAH.

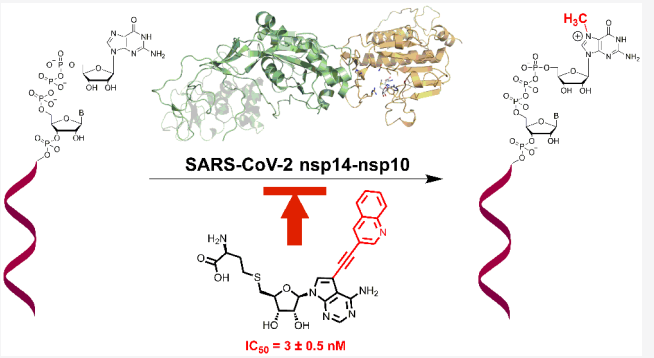

KEYWORDS: *COVID-19, SARS-CoV-2, methyltransferase, nsp14 nsp10, structure-based design, inhibitors*

COVID-19 and its causative agent, the SARS-CoV-2 virus, dominated the public debate last year.[1] The virus first emerged in Wuhan, China, and quickly spread around the world, causing a worldwide pandemic.[2] The vaccines have been developed at an amazing pace, and vaccination has already started in several countries.[3] However, only one small-molecule drug, remdesivir,[4,5] a broad-spectrum RNA-dependent RNA polymerase inhibitor,[6−8] is currently fully approved for treatment of COVID-19, but small-molecule drugs are urgently needed for people who, for various reasons, cannot be vaccinated or become sick before or despite vaccination. SARS-CoV-2 and other coronaviruses have an unusually large genome (~30 000 bp) for single-stranded positive-sense RNA viruses.[2,9] They encode 4 structural, 16 nonstructural (nsp1−16), and several accessory proteins.[10,11] Among these, enzymes are the best potential drug targets. Coronaviruses encode two proteases, RNA-dependent RNA polymerase (RdRp), helicase, endonuclease, and two MTases.[12,13] Each of these is a valid drug target, as inhibition of any of them would be lethal for the virus. Several inhibitors of SARS-CoV-2 RdRp and the main protease that have drug-like properties have recently been described.[14−16]

Here, we have focused on the nsp14 protein with two enzymatic activities: the N-terminal domain has 3′-to-5′ exoribonuclease (ExoN) activity, while the C-terminal domain has N7-MTase activity.[10,17,18] The ExoN activity is critical for the maintenance of the large RNA genome,[17] whereas the MTase activity is important for the stability of viral RNAs. Nsp14 uses SAM as a methyl donor to methylate the N7 position of 5′ guanine, one of the steps to build the cap that is essential for mRNA stability and translation in human cells. We have used a structure-guided approach to design molecules with the potential to inhibit the nsp14 MTase activity. Several of the compounds exhibited single-digit nanomolar activities in biochemical assays.

Most of SARS-CoV-2 enzymes have been quickly structurally characterized, but nsp14 still resists crystallographic analysis. Therefore, we have constructed a model of SARS-CoV-2 in complex with SAM based on its high homology (94.9% sequence identity) with the crystallized SARS-CoV nsp14.[19] We have based the design of our inhibitors on the molecular structure of SAH, a byproduct of the methylation reaction catalyzed by this protein. We have focused in particular on the interaction of such derivatives with lipophilic residues and residues potentially forming noncovalent

Received: March 15, 2021

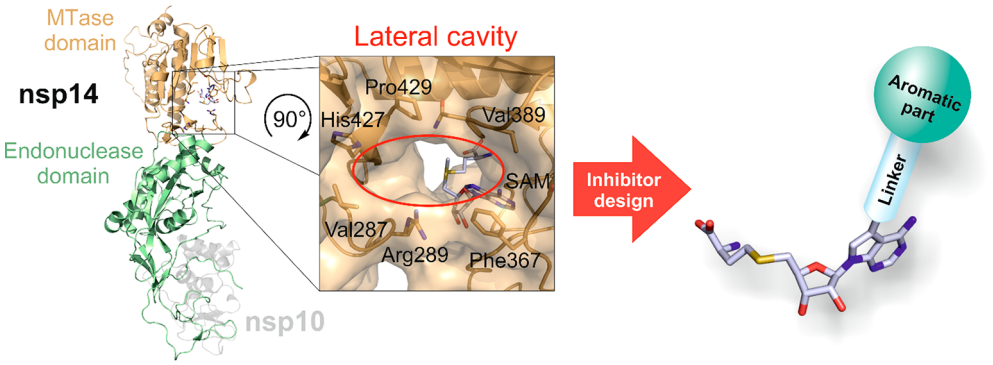

Figure 1. Homology model of nsp14 in complex with its activator protein nsp10 shows a well-defined lateral cavity in close proximity to the SAM/SAH binding site of the nsp14 MTase domain. This cavity is adjacent to the N7 position of the purine nucleobase and thus can be targeted by SAH derivatives bearing an aromatic substituent attached to this position by various linkers.

Scheme 1[a]

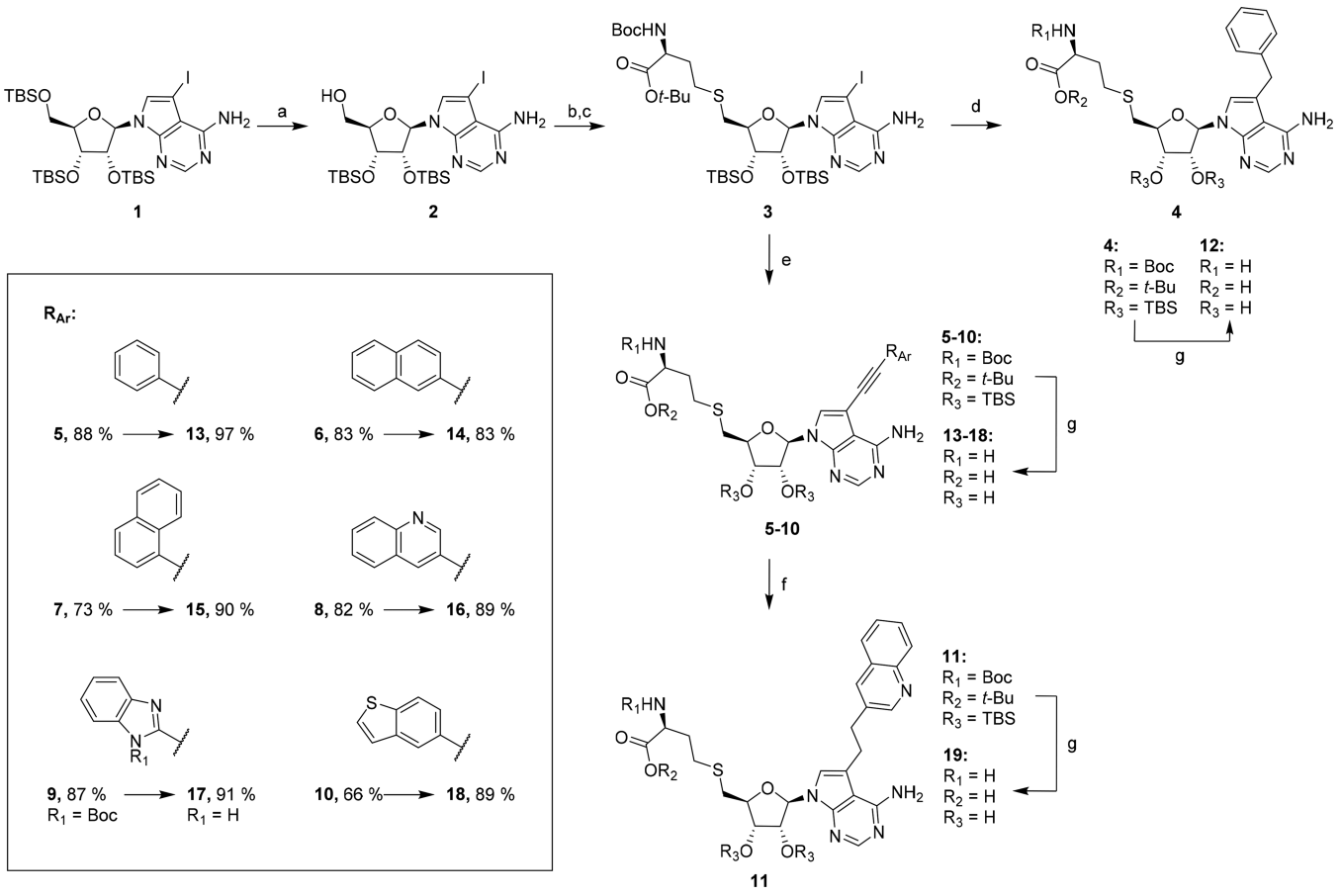

[a]Reagents and conditions: (a) CCl_3COOH, THF/H_2O, 0 °C, 72%. (b) MsCl, Et_3N, CH_2Cl_2, 0 °C to r.t. (c) *tert*-butyl (*tert*-butoxycarbonyl)-L-homocysteinate, *t*-BuOK, NMP, r.t., 82% after 2 steps. (d) Benzylzinc bromide, $Pd_2(dba)_3$, Xantphos, THF, 60 °C. (e) (Het)aryl acetylene, $Pd(PPh_3)_4$, CuI, Et_3N, THF, 60 °C (f) Prepared from **8**, Pd/C−H_2, EtOAc/EtOH, r.t. (g) TFA/H_2O (9:1), r.t.

interactions with π-systems within a lateral cavity revealed by manual inspection of the homology model. The cavity is defined by several hydrophobic residues (Val287, Phe367, Val389, Pro429) and Arg289, the last of which nicely closes the cavity by an interaction with the benzene ring of Phe367 (Figure 1). The size of the cavity in this region suggests that it is able to accommodate a relatively large planar substituent, which can significantly reduce the hydrophilic character of the ligand:nsp14 interaction and lead to a considerable increase in this interaction. We thus decided to use aromatic systems connected by appropriate linkers to position 7 of the 7-deazaadenine derivative of SAH (Figure 1). We selected methylene, ethynediyl, and ethylene as suitable linkers for the connection of aromatic parts to the nucleobase. We hypothesized that selected aromatic systems could significantly interact with both aromatic amino acid residues and Arg289 through the cation-π interaction, which had been observed for numerous interactions between ligands and proteins. Therefore, in most cases, we chose aromatic systems composed of two aromatic rings that provided large enough π electron

https://doi.org/10.1021/acsinfecdis.1c00131
ACS Infect. Dis. XXXX, XXX, XXX−XXX

clouds. Various aromatic systems bearing both hydrophilic and hydrophobic substituents were prepared in our study, and the most active derivatives were selected for presentation.

Synthesis of the Designed Nsp14 Inhibitors. The starting compound for the synthesis of the designed nsp14 inhibitors was persilylated 7-deaza-7-iodoadenosine **1**.[20,21] First, the silyl-protecting group attached at the 5′-position was selectively removed by treatment with trichloroacetic acid affording nucleoside **2** in 72% yield.[22] Activation of the 5′-hydroxy group of the compound **2** with MsCl in the presence of Et_3N allowed to introduce an amino acid moiety by nucleophilic substitution with freshly prepared protected L-homocysteine salt[23,24] yielding SAH analogue **3** (82% after two steps). This key intermediate **3** was then subjected to cross-coupling reactions to attach hetaryl and aryl substituents through various linkers. For the preparation of the analogue with a methylene bridge, the Negishi cross-coupling reaction with benzylzinc bromide in the presence of Pd_2dba_3 and Xantphos was used affording compound **4** in 81% yield. Derivatives **5**−**10** with an ethynediyl bridge were prepared via Sonogashira cross-coupling reactions[25] with various (het)aryl acetylenes (for the synthesis, see SI) using a combination of $Pd(PPh_3)_4$ and CuI as a catalyst. In the case of compound **8** bearing quinoline substituent, its analogue **11** with ethylene linker was synthesized via reduction of the ethynediyl bridge by catalytic hydrogenation on Pd/C.[25] Final deprotection of 7-substituted SAH analogues **4**−**11** under acidic conditions (TFA/water 9:1) afforded the target compounds **12**−**19** in very good to excellent yields (83−97%, Scheme 1).

Assessment of the Potency of Nsp14 Inhibitors. A recently developed radioactivity-based nsp14 MTase assay[26] was employed to evaluate the inhibitory effect of compounds **12**−**19**. To our delight, all eight compounds inhibited nsp14 MTase activity with IC_{50} values ranging from 3 to 37 nM (Table 1 and SI, Figure S1a). Compound **16** was the most potent with the IC_{50} value of 3 ± 0.5 nM (Figure 2a, Table 1). Sinefungin (SIN) was used as a control with IC_{50} value of 18.2 ± 1.4 nM (Figure S1c, Table 1). To confirm the binding of these potent inhibitors to nsp14 orthogonally, we employed surface plasmon resonance (SPR). Strong binding of all eight compounds to nsp14 was observed (Table 1, SI, Figure S1b); the calculated K_D values from steady-state affinity fitting were in the range of 11−116 nM (Figure 2b,c, Table 1). However, the compounds did not completely dissociate in between injections. Testing compound **16** using multicycle kinetics (Figure S2) also indicated binding with a K_D value of 17.9 ± 2.5 nM, which is comparable with the K_D value from single-cycle kinetic SPR (25.2 ± 2.4; Table 1). Our data indicate that the compounds may have a relatively longer residence time. Binding affinities were in good agreement with the pattern of their inhibitory effect on nsp14 MTase activity (Table 1). The mechanism of action (MOA) of compounds **15** and **16** were further investigated and showed that both derivatives are SAM competitive, but RNA noncompetitive nsp14 inhibitors (Figure S3). Since SAM is a very common methyl donor in methylation reactions, we evaluated the selectivity of compound **15** and **16** against a panel of 33 human RNA-, DNA-, and protein- MTases (Table S1). No significant inhibitory effect was observed for 20 protein lysine-MTases, PRMT5 and PRMT9. However, both compounds inhibited the MTase activity of type I PRMTs, PRMT7, and DNMTs. In particular, compound **15** inhibited DOT1L, DNMT3A/3L, DNMT3B/3L with IC_{50} 56, 9, and 26 nM, respectively, whereas compound **16** exerted inhibition of the same with IC_{50} values of 5, 10, and 30 nM, respectively (Figure S4, Table S2). We also tested both compounds for selectivity against human RNMT, which has a similar function as nsp14. Compound **15** and **16** inhibited RNMT with IC_{50} values of 700 and 500 nM, indicating an excellent selectivity of these compounds against the human counterpart (Figure S5).

Table 1. Evaluation of the Binding Affinity and Inhibitory Effect of the Designed Compounds[a]

compound	IC_{50} (nM)	Hill slope	K_D (nM)	score (Gold)
12	37 ± 7	0.7	31.2 ± 0.9	95.87
13	11 ± 1	0.8	14.1 ± 0.7	100.93
14	17 ± 3	0.8	116 ± 7.7	108.40
15	6 ± 1	0.8	21.6 ± 1.3	110.89
16	3 ± 0.5	0.9	25.2 ± 2.4	99.02
17	4 ± 0.5	0.9	15.1 ± 0.3	101.42
18	15 ± 3	0.7	11.3 ± 0.9	102.01
19	12 ± 1	0.8	23.1 ± 1.0	108.91
SIN	18 ± 2	0.7	ND	87.71
SAH[b]	130 ± 30	0.7	ND	85.96

[a]All values come from the data presented in Figure 2 (n = 3) and Figure S1. [b]The IC_{50} value for SAH was identical with ref 26.

Docking Studies of the Inhibitors Obtained. In order to corroborate our observations in enzymatic assays, we used our homology model and performed molecular docking of selected compounds from our study. The homology model was prepared using SWISS-MODEL server[27] based on the crystal structure of nsp14 in complex with nsp10 obtained for SARS-CoV by Ma et al. (PDB ID: 5C8T).[19] The SAM-binding site and the position of the ligand were optimized, and four water molecules in the immediate vicinity of the amino acid part of the SAM molecule were modeled in order to stabilize this flexible part of our SAH analogues during the docking experiments. The 3D structures of the ligands were optimized using MOPAC 2016[28] prior to docking. The homology model of the protein was processed using the standard procedure for the GOLD software,[29] which was selected as the most suitable software for the docking of SAM/SAH analogues based on our previous experience and initial docking experiments. In all cases, the docking experiments in the GOLD software resulted in the highest scores ranging from 95.9 (for compound **12**) to 110.9 (compound **15**) for the poses that orient the aromatic parts into the lateral cavity defined above (Table 1 and SI, Figure S6). We have decided to present the binding patterns of the compounds that are of interest and may lead to further improvements in these inhibitors (Figure 3). Interestingly, the compound with the lowest IC_{50} (derivative **16**) gave only an average score (99.0, Figure 3, A and B) as did the compound **18**, which exhibited the highest affinity in the SPR assay (102.0, Figure 3, C and D). In contrast, the compound with the third lowest IC_{50} value, derivative **15**, scored the best in GOLD (110.9, Figure 3, E and F). The 1-naphthyl moiety of this compound seems to occupy very nicely the lateral cavity of nsp14. We have also obtained an interesting docking result for the compound **13**, which exhibits relatively high activity in both IC_{50} and SPR assays. The docking results show that the aromatic core can also be located in the lateral cavity perpendicular to the rotation of this part in other compounds. This can be attributed to the less lipophilic nature of the benzimidazole moiety in comparison with the other sub-

https://doi.org/10.1021/acsinfecdis.1c00131
ACS Infect. Dis. XXXX, XXX, XXX−XXX

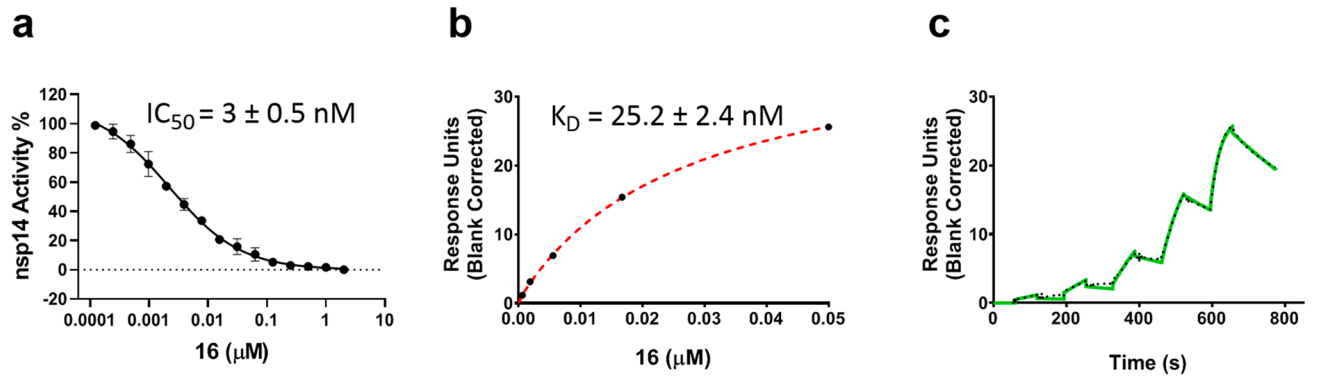

Figure 2. Characterization of compound **16**. (a) Concentration-dependent nsp14 MTase inhibition by compound **16** was assessed using the radioactivity-based assay. The binding of compound **16** to nsp14 was tested by SPR. (b) The steady-state response (black circles) with the steady-state 1:1 binding model fitting (red dashed line) and (c) the sensorgram (solid green) with the kinetic fit (black dots) are shown. The experiments were performed in triplicate.

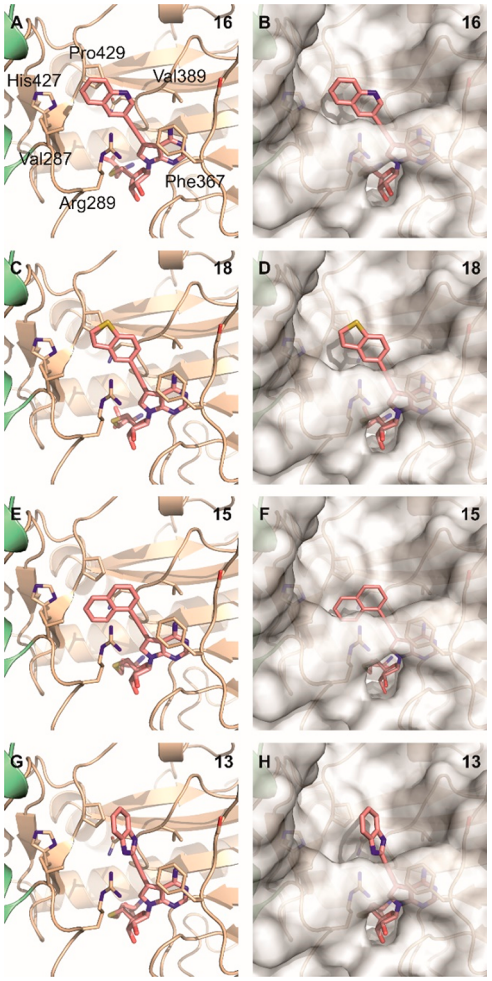

Figure 3. Results of the docking studies of compounds **16** (A and B), **18** (C and D), **15** (E and F), and **13** (G and H) using the homology model of SARS-CoV-2 nsp14 MTase.

stituents used (Figure 3, G and H). We can only speculate that these discrepancies between the actual activity and the predicted docking scores can be attributed to the small differences between the obtained activities and affinities of the inhibitors, imperfections in the homology model, flexibilities of lateral-cavity residues (e.g., Arg289, Phe367, and Asn388), and/or further water-mediated contacts with the nsp14 protein. We tried to address this problem by molecular modeling at the semiempirical quantum mechanical level of theory, which showed that compound **16** had considerably more favorable binding free energy than SAH, due to the interaction with key Phe367, Asn388, and Pro429 residues in the lateral pocket (Figure S7). From the point of view of the structure−activity relationship, our data, results of docking studies, and molecular modeling show several facts. First, the installation of a lipophilic substituent leads to a significant increase in the activity of SAH derivatives, which is clear also from the molecular modeling and the docking studies. Second, derivatives that have a methylene bridge are significantly less active than derivatives that have a lipophilic substituent linked to the deazapurine nucleobase via a triple bond both in vitro and in silico (Table 1, compound **12** vs **13**). These derivatives are also more active than their counterparts containing a saturated ethylene bond (Table 1, compound **16** vs **19**). Finally, derivatives bearing bicyclic lipophilic substituents have comparable activity to each other.

In conclusion, this study describes the first rationally designed inhibitors of nsp14 MTase, based on modified derivatives of the SAH molecule. In order to effectively target the lateral cavity of the enzyme, which directly communicates with the SAM/SAH-binding site, we used the 7-deazaadenine analogue of SAH. This allowed us to attach aromatic substituents to position 7 using appropriate linkers. These derivatives showed considerable inhibitory activity against nsp14 (the IC_{50} values were between 3 and 37 nM) and strong binding to the nsp14 protein by SPR (with the K_D values being in the range of 11−31 nM). The most active compound in the study was compound **16** (TO507) with IC_{50} = 3 ± 0.5 nM. Our docking and molecular modeling studies have clearly shown that these compounds can effectively exploit the space within the lateral cavity, which leads to effective binding to the SAM-binding site of the protein. Although the compounds are inherently zwitterionic, and hence their penetration into cells and their activity in cell cultures are rather unlikely, we believe that our study provides a significant springboard for the design of drugs targeting the nsp14 protein.

METHODS

Methyltransferase Assay. Inhibitory effect of all compounds was assessed using a recently developed radioactivity-based nsp14 methyltransferase assay.[26] In this assay, the transfer of the ^{3}H-methyl group from ^{3}H-SAM to guanine-N7

https://doi.org/10.1021/acsinfecdis.1c00131
ACS Infect. Dis. XXXX, XXX, XXX−XXX

was monitored using Scintillation Proximity Assay (SPA). The enzymatic reactions were performed at 23 °C with 20 min incubation of 20 μL reaction mixture in 20 mM Tris pH 8.0, 0.25 mM $MgCl_2$, 0.01% Triton X-100 containing 0.25 μM of ^{3}H-SAM (Cat.# NET155 V250UC; PerkinElmer; www.perkinelmer.com), 0.05 μM of biotinylated-RNA, 1.5 nM nsp14, and compound titrations. To stop the reactions, 20 μL of 7.5 M Guanidine hydrochloride was added, followed by 40 μL of buffer (20 mM Tris, pH 8.0), mixed and transferred to a 384-well Streptavidin coated Flash-plate (PerkinElmer, http://www.perkinelmer.ca). After mixing, the mixtures in Flash-plate were incubated for 2 h and the CPM counts were measured using Topcount plate reader (PerkinElmer, www.perkinelmer.com). The CPM counts in the absence of compound for each data set were defined as 100% activity. In the absence of the enzyme, the CPM counts in each data set were defined as background (0%). All enzymatic reactions were performed in triplicate, and IC_{50} values were determined by fitting the data to Four Parameter Logistic equation using GraphPad Prism 7 software.

Surface Plasmon Resonance. Binding affinities of compounds were assessed by Surface Plasmon Resonance (SPR) using a Biacore T200 from GE Healthcare. Nsp14 (aa 1−527) and SETD3 (aa 1−605, as control) were coupled on a CM5 SPR Sensor chip (GE healthcare) separately. Compounds were injected into the sensitized chip at 5 different concentrations in 0.5% DMSO at 50 μL/min, using HBS-EP Plus buffer (10 mM HEPES pH 7.4, 150 mM NaCl, 2 mM EDTA, 0.005% Tween 20). Contact time was 60 s, and disassociation time was 120 s. Buffer alone (plus 0.5% DMSO) was used for blank injections, and buffers containing 0.4 to 0.6% DMSO were used for buffer corrections. For multicycle kinetics, association time was 60 s, dissociation was 180 s, and 6 different concentrations of compound **16** were used from 0.003 to 0.66 μM.

■ ASSOCIATED CONTENT

Supporting Information

The Supporting Information is available free of charge at https://pubs.acs.org/doi/10.1021/acsinfecdis.1c00131.

Synthetic procedures, methods for docking studies and molecular modeling; Supporting figures and tables; ^{1}H and ^{13}C NMR of new compounds and HPLC purity of final SAH analogues (PDF)

■ AUTHOR INFORMATION

Corresponding Authors

Masoud Vedadi − *Structural Genomics Consortium and Department of Pharmacology and Toxicology, University of Toronto, Toronto, Ontario M5G 1L7, Canada;* orcid.org/0000-0002-0574-0169; Email: m.vedadi@utoronto.ca

Evzen Boura − *Institute of Organic Chemistry and Biochemistry, Czech Academy of Sciences, v.v.i., Gilead Sciences Research Centre at the IOCB Prague, 166 10 Prague 6, Czech Republic;* orcid.org/0000-0002-9652-4065; Email: evzen.boura@uochb.cas.cz

Radim Nencka − *Institute of Organic Chemistry and Biochemistry, Czech Academy of Sciences, v.v.i., Gilead Sciences Research Centre at the IOCB Prague, 166 10 Prague 6, Czech Republic;* orcid.org/0000-0001-6167-0380; Email: nencka@uochb.cas.cz

Authors

Tomáš Otava − *Institute of Organic Chemistry and Biochemistry, Czech Academy of Sciences, v.v.i., Gilead Sciences Research Centre at the IOCB Prague, 166 10 Prague 6, Czech Republic; Faculty of Food and Biochemical Technology, University of Chemistry and Technology, 166 28 Prague 6, Czech Republic*

Michal Šála − *Institute of Organic Chemistry and Biochemistry, Czech Academy of Sciences, v.v.i., Gilead Sciences Research Centre at the IOCB Prague, 166 10 Prague 6, Czech Republic*

Fengling Li − *Structural Genomics Consortium, University of Toronto, Toronto, Ontario M5G 1L7, Canada*

Jindřich Fanfrlík − *Institute of Organic Chemistry and Biochemistry, Czech Academy of Sciences, v.v.i., Gilead Sciences Research Centre at the IOCB Prague, 166 10 Prague 6, Czech Republic*

Kanchan Devkota − *Structural Genomics Consortium, University of Toronto, Toronto, Ontario M5G 1L7, Canada*

Sumera Perveen − *Structural Genomics Consortium, University of Toronto, Toronto, Ontario M5G 1L7, Canada*

Irene Chau − *Structural Genomics Consortium, University of Toronto, Toronto, Ontario M5G 1L7, Canada*

Paknoosh Pakarian − *Structural Genomics Consortium, University of Toronto, Toronto, Ontario M5G 1L7, Canada*

Pavel Hobza − *Institute of Organic Chemistry and Biochemistry, Czech Academy of Sciences, v.v.i., Gilead Sciences Research Centre at the IOCB Prague, 166 10 Prague 6, Czech Republic;* orcid.org/0000-0001-5292-6719

Complete contact information is available at: https://pubs.acs.org/10.1021/acsinfecdis.1c00131

Author Contributions

T.O. and M.Š., design and synthesis of the final compounds; F.L., K.D., S.P., I.C., and P.P., biochemical assays; J.F. and P.H., molecular modeling; M.V., E.B., and R.N., study design, manuscript conception, and writing.

Notes

The authors declare the following competing financial interest(s): Part of the study was supported by Gilead Sciences, Inc.

■ ACKNOWLEDGMENTS

We acknowledge Katerina Millerova for critical reading of the text. We used PYMOL software[30] to prepare the figures both in the main text and SI. The work was supported from the European Regional Development Fund; OP RDE; Project: "Chemical Biology for Drugging Undruggable Targets (ChemBioDrug)" (No. CZ.02.1.01/0.0/0.0/16_019/0000729). We acknowledge the support from the Ministry of Health of the Czech Republic, Grant NU20-05-00472 and the Czech Academy of Sciences (RVO: 61388963). A part of the study was also supported by Gilead Sciences, Inc. Masoud Vedadi was supported by the University of Toronto COVID-19 Action Initiative-2020 funds, and COVID-19 Mitacs Accelerate postdoctoral award to Sumera Perveen. The Structural Genomics Consortium is a registered charity (No. 1097737) that receives funds from AbbVie, Bayer Pharma AG, Boehringer Ingelheim, Canada Foundation for Innovation, Eshelman Institute for Innovation, Genentech, Genome Canada through Ontario Genomics Institute [OGI-196], EU/EFPIA/OICR/McGill/KTH, Diamond Innovative Medi-

cines Initiative 2 Joint Undertaking [EUbOPEN Grant 875510], Janssen, Merck KGaA (a.k.a. EMD in Canada and US), Merck & Co. (a.k.a. MSD outside Canada and US), Pfizer, São Paulo Research Foundation-FAPESP, Takeda and Wellcome [106169/ZZ14/Z]. We would like to thank Pegah Ghiabi, Taraneh Hajian, and Albina Bolotokova for technical support.

■ ABBREVIATIONS

SARS-CoV, severe acute respiratory syndrome-related coronavirus; COVID-19, coronavirus disease 2019; +RNA, single-stranded positive-sense RNA; RdRp, RNA-dependent RNA polymerase; ExoN, 3′-to-5′ exoribonuclease; MTase, methyltransferase; SAM, *S*-adenosyl-L-methionine; SAH, *S*-adenosyl-L-homocysteine.

■ REFERENCES

(1) Lai, C. C., Shih, T. P., Ko, W. C., Tang, H. J., and Hsueh, P. R. (2020) Severe acute respiratory syndrome coronavirus 2 (SARS-CoV-2) and coronavirus disease-2019 (COVID-19): The epidemic and the challenges. *Int. J. Antimicrob. Agents 55* (3), 105924.

(2) Chan, J. F. W., Kok, K. H., Zhu, Z., Chu, H., To, K. K. W., Yuan, S. F., and Yuen, K. Y. (2020) Genomic characterization of the 2019 novel human-pathogenic coronavirus isolated from a patient with atypical pneumonia after visiting Wuhan. *Emerging Microbes Infect. 9* (1), 221−236.

(3) Li, D. D., and Li, Q. H. (2021) SARS-CoV-2: vaccines in the pandemic era. *Mil. Med. Res.*, DOI: 10.1186/s40779-020-00296-y.

(4) Pruijssers, A. J., George, A. S., Schafer, A., Leist, S. R., Gralinksi, L. E., Dinnon, K. H., Yount, B. L., Agostini, M. L., Stevens, L. J., Chappell, J. D., Lu, X. T., Hughes, T. M., Gully, K., Martinez, D. R., Brown, A. J., Graham, R. L., Perry, J. K., Du Pont, V., Pitts, J., Ma, B., Babusis, D., Murakami, E., Feng, J. Y., Bilello, J. P., Porter, D. P., Cihlar, T., Baric, R. S., Denison, M. R., and Sheahan, T. P. (2020) Remdesivir Inhibits SARS-CoV-2 in Human Lung Cells and Chimeric SARS-CoV Expressing the SARS-CoV-2 RNA Polymerase in Mice. *Cell Rep. 32* (3), 107940.

(5) de Wit, E., Feldmann, F., Cronin, J., Jordan, R., Okumura, A., Thomas, T., Scott, D., Cihlar, T., and Feldmann, H. (2020) Prophylactic and therapeutic remdesivir (GS-5734) treatment in the rhesus macaque model of MERS-CoV infection. *Proc. Natl. Acad. Sci. U. S. A. 117* (12), 6771−6776.

(6) Agostini, M. L., Andres, E. L., Sims, A. C., Graham, R. L., Sheahan, T. P., Lu, X. T., Smith, E. C., Case, J. B., Feng, J. Y., Jordan, R., Ray, A. S., Cihlar, T., Siegel, D., Mackman, R. L., Clarke, M. O., Baric, R. S., and Denison, M. R. (2018) Coronavirus Susceptibility to the Antiviral Remdesivir (GS-5734) Is Mediated by the Viral Polymerase and the Proofreading Exoribonuclease. *mBio*, DOI: 10.1128/mBio.00221-18.

(7) Brown, A. J., Won, J. J., Graham, R. L., Dinnon, K. H., Sims, A. C., Feng, J. Y., Cihlar, T., Denison, M. R., Baric, R. S., and Sheahan, T. P. (2019) Broad spectrum antiviral remdesivir inhibits human endemic and zoonotic deltacoronaviruses with a highly divergent RNA dependent RNA polymerase. *Antiviral Res. 169*, 104541.

(8) Konkolova, E., Dejmek, M., Hrebabecky, H., Sala, M., Boserle, J., Nencka, R., and Boura, E. (2020) Remdesivir triphosphate can efficiently inhibit the RNA-dependent RNA polymerase from various flaviviruses. *Antiviral Res. 182*, 104899.

(9) Romano, M., Ruggiero, A., Squeglia, F., Maga, G., and Berisio, R. (2020) A Structural View of SARS-CoV-2 RNA Replication Machinery: RNA Synthesis, Proofreading and Final Capping. *Cells 9* (5), 1267.

(10) Snijder, E. J., Decroly, E., and Ziebuhr, J. (2016) The Nonstructural Proteins Directing Coronavirus RNA Synthesis and Processing. *Adv. Virus Res. 96*, 59−126.

(11) Ziebuhr, J. (2006) The coronavirus replicase: Insights into a sophisticated enzyme machinery. *Nidoviruses: toward Control of Sars and Other Nidovirus Diseases 581*, 3−11.

(12) Wu, Y. U., Li, Z., Zhao, Y. S., Huang, Y. Y., Jiang, M. Y., and Luo, H. B. (2021) Therapeutic targets and potential agents for the treatment of COVID-19. *Med. Res. Rev. 41*, 1775.

(13) Sarkar, K., Sil, P. C., Nabavi, S. F., Berindan-Neagoe, I., Cismaru, C. A., Nabavi, S. M., and Habtemariam, S. (2020) Possible Targets and Therapies of SARS-C V-2 Infection. *Mini-Rev. Med. Chem. 20* (18), 1900−1907.

(14) Yousefi, H., Mashouri, L., Okpechi, S. C., Alahari, N., and Alahari, S. K. (2021) Repurposing existing drugs for the treatment of COVID-19/SARS-CoV-2 infection: A review describing drug mechanisms of action. *Biochem. Pharmacol. 183*, 114296.

(15) Frediansyah, A., Tiwari, R., Sharun, K., Dhama, K., and Harapan, H. (2021) Antivirals for COVID-19: A critical review. *Clin. Epidemiol. Glob. Health 9*, 90−98.

(16) Kevadiya, B. D., Machhi, J., Herskovitz, J., Oleynikov, M. D., Blomberg, W. R., Bajwa, N., Soni, D., Das, S., Hasan, M., Patel, M., Senan, A. M., Gorantla, S., McMillan, J., Edagwa, B., Eisenberg, R., Gurumurthy, C. B., Reid, S. M., Punyadeera, C., Chang, L. D., and Gendelman, H. E. (2021) Pharmacotherapeutics of SARS-CoV-2 Infections. *J. Neuroimmune Pharmacol. 16*, 1−26.

(17) Minskaia, E., Hertzig, T., Gorbalenya, A. E., Campanacci, V., Cambillau, C., Canard, B., and Ziebuhr, J. (2006) Discovery of an RNA virus 3 ’→ 5 ’ exoribonuclease that is critically involved in coronavirus RNA synthesis. *Proc. Natl. Acad. Sci. U. S. A. 103* (13), 5108−5113.

(18) Ogando, N. S., Zevenhoven-Dobbe, J. C., van der Meer, Y., Bredenbeek, P. J., Posthuma, C. C., and Snijder, E. J. (2020) The Enzymatic Activity of the nsp14 Exoribonuclease Is Critical for Replication of MERS-CoV and SARS-CoV-2. *J. Virol.*, DOI: 10.1128/JVI.01246-20.

(19) Ma, Y. Y., Wu, L. J., Shaw, N., Gao, Y., Wang, J., Sun, Y. N., Lou, Z. Y., Yan, L. M., Zhang, R. G., and Rao, Z. H. (2015) Structural basis and functional analysis of the SARS coronavirus nsp14-nsp10 complex. *Proc. Natl. Acad. Sci. U. S. A. 112* (30), 9436−9441.

(20) Zhang, L., Zhang, Y., Li, X., and Zhang, L. (2002) Study on the Synthesis and PKA-I Binding Activities of 5-Alkynyl Tubercidin Analogues. *Bioorg. Med. Chem. 10* (4), 907−912.

(21) Bourderioux, A., Nauš, P., Perlíková, P., Pohl, R., Pichová, I., Votruba, I., Džubák, P., Konečný, P., Hajdúch, M., Stray, K. M., Wang, T., Ray, A. S., Feng, J. Y., Birkus, G., Cihlar, T., and Hocek, M. (2011) Synthesis and Significant Cytostatic Activity of 7-Hetaryl-7-deazaadenosines. *J. Med. Chem. 54* (15), 5498−5507.

(22) Zhu, X.-F., Williams, H. J., and Ian Scott, A. (2003) Aqueous Trichloroacetic Acid: Another Useful Reagent for Highly Selective 5′-Desilylation of Multisilylated Nucleosides. *Synth. Commun. 33* (12), 2011−2016.

(23) Zhu, J., Hu, X., Dizin, E., and Pei, D. (2003) Catalytic Mechanism of S-Ribosylhomocysteinase (LuxS): Direct Observation of Ketone Intermediates by 13C NMR Spectroscopy. *J. Am. Chem. Soc. 125* (44), 13379−13381.

(24) Bourdier, T., Fookes, C. J. R., Pham, T. Q., Greguric, I., and Katsifis, A. (2008) Synthesis and stability of S-(2-[18F]fluoroethyl)-L-homocysteine for potential tumour imaging. *J. Labelled Compd. Radiopharm. 51* (11), 369−373.

(25) Ondruš, M., Sýkorová, V., Bednárová, L., Pohl, R., and Hocek, M. (2020) Enzymatic synthesis of hypermodified DNA polymers for sequence-specific display of four different hydrophobic groups. *Nucleic Acids Res. 48* (21), 11982−11993.

(26) Devkota, K., Schapira, M., Perveen, S., Yazdi, A. K., Li, F., Chau, I., Ghiabi, P., Hajian, T., Loppnau, P., Bolotokova, A., Satchell, K. J. F., Wang, K., Li, D., Liu, J., Smil, D., Luo, M., Jin, J., Fish, P. V., Brown, P. J., and Vedadi, M. (2021) Probing the SAM Binding Site of SARS-CoV-2 nsp14 in vitro Using SAM Competitive Inhibitors Guides Developing Selective bi-substrate Inhibitors. *SLAS Discovery*, DOI: 10.1101/2021.02.19.424337.

https://doi.org/10.1021/acsinfecdis.1c00131
ACS Infect. Dis. XXXX, XXX, XXX−XXX

(27) Waterhouse, A., Bertoni, M., Bienert, S., Studer, G., Tauriello, G., Gumienny, R., Heer, F. T., de Beer, T. A. P., Rempfer, C., Bordoli, L., Lepore, R., and Schwede, T. (2018) SWISS-MODEL: homology modelling of protein structures and complexes. *Nucleic Acids Res. 46* (W1), W296−W303.
(28) Stewart, J. J. P. (2012) *MOPAC2012*, Version 7.263W. http://openmopac.net (accessed Jun 5, 2021).
(29) Jones, G., Willett, P., Glen, R. C., Leach, A. R., and Taylor, R. (1997) Development and validation of a genetic algorithm for flexible docking. *J. Mol. Biol. 267* (3), 727−748.
(30) Schrodinger, LLC (2010) *PyMOL Molecular Graphics System*, Version 1.8.

https://doi.org/10.1021/acsinfecdis.1c00131
ACS Infect. Dis. XXXX, XXX, XXX−XXX